

# Lawrence Berkeley National Laboratory

## Lawrence Berkeley National Laboratory

### **Title**

Enhanced Magnetism of Fe<sub>3</sub>O<sub>4</sub> Nanoparticles with Ga Doping

### **Permalink**

<https://escholarship.org/uc/item/3621q2w6>

### **Author**

Pool, V. L.

### **Publication Date**

2011-04-05

Peer reviewed

# Enhanced magnetism of Fe<sub>3</sub>O<sub>4</sub> nanoparticles with Ga doping

V. L. Pool,<sup>1,a)</sup> M. T. Klem,<sup>2,3</sup> C. L. Chorney,<sup>2,3</sup> E. A. Arenholz,<sup>4</sup> and Y. U. Idzerda<sup>1</sup>

<sup>1</sup>*Department of Physics, Montana State University, Bozeman, Montana 59715, USA*

<sup>2</sup>*Department of Chemistry and Geochemistry, Montana Tech, Butte, Montana 59701, USA*

<sup>3</sup>*Center for Advanced Supramolecular and Nano Systems, Montana Tech, Butte, Montana 59715, USA*

<sup>4</sup>*Advanced Light Source, Lawrence Berkeley National Laboratory, Berkeley, California 94720, USA*

Magnetic (Ga<sub>x</sub>Fe<sub>1-x</sub>)<sub>3</sub>O<sub>4</sub> nanoparticles with 5%–33% gallium doping ( $x = 0.05$ – $0.33$ ) were measured using x-ray absorption spectroscopy and x-ray magnetic circular dichroism to determine that the Ga dopant is substituting for Fe<sup>3+</sup> as Ga<sup>3+</sup> in the tetrahedral A-site of the spinel structure, resulting in an overall increase in the total moment of the material. Frequency-dependent alternating-current magnetic susceptibility measurements showed these particles to be weakly interacting with a reduction of the cubic anisotropy energy term with Ga concentration. The element-specific dichroism spectra show that the average Fe moment is observed to increase with Ga concentration, a result consistent with the replacement of A-site Fe by Ga.

## I. INTRODUCTION

Gallium doped iron oxide, (Ga<sub>x</sub>Fe<sub>1-x</sub>)<sub>3</sub>O<sub>4</sub>, is interesting as it exhibits an energy-dependent photoabsorption as a function of Ga concentration in bulk samples.<sup>1</sup> This property could be advantageous in nanoparticles providing utility for applications. Additionally, Ga-based mixed oxides have shown interesting catalytic behavior, an application that nanoparticles are known to be exceptional for due to their large surface-to-volume ratio.<sup>2–4</sup> Furthermore, the doping of magnetic nanoparticles can have behaviors distinct from bulk alloys, including changes in dopant site occupation and different variations of moment and anisotropy with doping concentration, making them interesting from a purely scientific standpoint.

Bulk (Ga<sub>x</sub>Fe<sub>1-x</sub>)<sub>3</sub>O<sub>4</sub> magnetic trends have not been fully studied, but Ga is typically present as a 3+ valence ion so it is likely to be present as a 3+ valence ion given the two options in the spinel structure.<sup>1</sup> The effect on the magnetic properties of doping Fe<sub>3</sub>O<sub>4</sub> with other nonmagnetic transition metals of similar ionic radii, such as Zn, show that Zn preferentially substitutes for Fe<sup>3+</sup> as Zn<sup>2+</sup> in the tetrahedral coordination. For bulk Zn doped Fe<sub>3</sub>O<sub>4</sub> the total moment per unit cell increases as the tetrahedral sites become occupied by the nonmagnetic transition metal.<sup>5</sup> These substitutional atoms no longer partially cancel the Fe moment in the octahedral coordination. For Zn doping the average moment of the octahedral Fe sites also slightly increases as charge neutrality requires that some of the octahedral Fe<sup>2+</sup> convert to Fe<sup>3+</sup>. If Ga substitutes into the tetrahedral coordination as a Ga<sup>3+</sup> ion (rather than Zn<sup>2+</sup>), it should produce a similar, though slightly reduced effect.

Nanoparticles do not always follow the same trends as the bulk. Properties are often size dependent where surface effects and the relaxation of crystal lattice distortions can

cause nanoparticles to have distinctly different magnetic properties.<sup>6,7</sup> In addition, nanoparticles are notoriously synthesis dependent, while a chemically gentle nanoparticle synthesis process like protein encapsulation may generate one behavior, a harsher chemical process may show an entirely different behavior.<sup>8</sup> In particular, encapsulation of Zn nanoparticles in protein structures does result in substitution of Zn to the tetrahedral A-site, but generates a distinctly different magnetic behavior, characterized by a steep reduction in nanoparticle moment with Zn concentration, opposite the bulk behavior.<sup>9</sup> From simple crystal filling arguments, the reduced ion radius of Ga<sup>3+</sup> in comparison to Zn<sup>2+</sup> suggests that the Ga dopant should more strongly prefer the tetrahedral coordinated site than Zn, allowing for a further investigation of the peculiar moment behavior.

## II. EXPERIMENTAL PROCEDURES

In this study, magnetic (Ga<sub>x</sub>Fe<sub>1-x</sub>)<sub>3</sub>O<sub>4</sub> nanoparticles with 5%–33% gallium doping ( $x = 0.05$ – $0.33$ ) were synthesized by mixing Fe(acac)<sub>3</sub>, 1,2-hexadecanediol, benzyl ether, oleic acid, and oleylamine under evacuated conditions. The Fe<sub>3</sub>O<sub>4</sub> (magnetite) nanoparticles were synthesized by combining Fe(acac)<sub>3</sub> (0.5 mmol), oleic acid (1.5 mmol), oleylamine (1.5 mmol), 1,2-hexadecanediol (2.5 mmol), and benzyl ether (5 mL) in a 50 mL roundbottom flask under vacuum. The mixture was gradually heated to 200 °C and allowed to anneal for 24 h. The reaction mixture was then cooled to room temperature, and the particles were precipitated in ethanol, centrifuged, and dried. Gallium doped magnetite nanoparticles, (Ga<sub>x</sub>Fe<sub>1-x</sub>)<sub>3</sub>O<sub>4</sub> were synthesized by substitution of Ga(acac)<sub>3</sub> for the Fe(acac)<sub>3</sub>. TEM measurements determined their size to be 8.5–9 nm.

Investigation of the composition, electronic structure, and magnetic properties were accomplished using x-ray absorption spectroscopy (XAS) and x-ray magnetic circular dichroism (XMCD). These measurements, performed on beamline 4.0.2

and 6.3.1 of the Advanced Light Source (ALS) of the Lawrence Berkeley National Laboratories, give element-specific information with high sensitivity and strong magnetic contrast and have been used to identify doping positions and electronic valence of doped magnetic nanoparticles in the past.<sup>9–11</sup>

For these nanoparticles, samples were dried onto Formvar coated TEM grids and measured primarily in the electron yield configuration, though supplemental measurements were done in the transmission geometry. XAS was performed on the Fe and Ga  $L_{2,3}$  edges to determine the valence of the elements and the substitutional site of Ga. XMCD was performed on the Fe  $L_3$  edge to determine the moment per iron atom. XMCD measurements were done both at room temperature and at approximately 20 K with applied fields ranging from 0.5 to 1 T using 90% polarized light. For comparison, measurements were done on  $\beta$ -phase  $\text{Ga}_2\text{O}_3$  acquired as a powder standard from Alfa Aesar.

To determine if the particles are interacting with one another, temperature-dependent, alternating-current magnetic susceptibility (ACMS) measurements were performed over a range of frequencies from 178 to 10,000 Hz using a Quantum Design Physical Property Measurement System (PPMS).

### III. RESULTS AND DISCUSSION

A standard Neel–Arrhenius plot of the frequency-dependent ACMS data was created for various Ga concentrations (not shown). The negative natural log of the frequency was plotted as a function of the inverse of the blocking temperature (the peak in the real part of the susceptibility curve) over a range of frequencies from 178 to 10,000 Hz. A straight-line fit of the data was found to be unsatisfactory, suggesting that these bare nanoparticles are slightly interacting. The interaction is significant enough that it is not possible to reliably extract the quantitative anisotropy energies and the attempt frequencies from the ACMS data, although

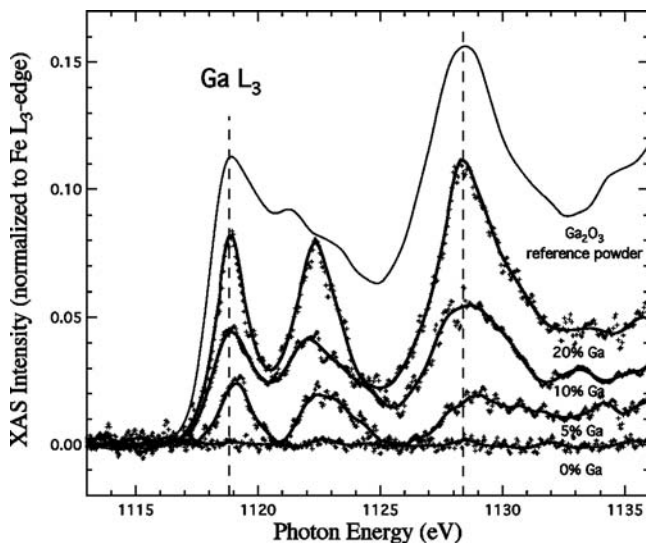


FIG. 1. The Ga  $L_3$ -edge XAS spectra for  $(\text{Ga}_x\text{Fe}_{1-x})_3\text{O}_4$  with  $x = 0, 0.05, 0.1,$  and  $0.2$ . The points are single scans and the solid lines are the average of multiple scans. The spectra are normalized to the Fe  $L_3$ -edge XAS peak intensity for each scan. Also shown is an arbitrarily normalized single scan of the Ga  $L_3$ -edge spectrum for  $\beta$ -phase  $\text{Ga}_2\text{O}_3$  reference powder.

the trend of the ACMS data is toward reduced anisotropy with increasing Ga content.

By comparing the evolution of the Ga  $L_3$  XAS spectra to that of a  $\beta$ -phase  $\text{Ga}_2\text{O}_3$  reference powder (shown in Fig. 1), the  $L_3$  peak energies (dashed line at 1118.9 eV) are found to correspond nearly exactly, suggesting that the Ga is substituting into the host lattice as a 3+ cation. The Ga XAS of the  $(\text{Ga}_x\text{Fe}_{1-x})_3\text{O}_4$  are normalized to the Fe  $L_3$  XAS intensity of each scan so that the relative intensities can be used to confirm the target Ga concentration percentages. The  $\beta$ - $\text{Ga}_2\text{O}_3$  reference spectrum is arbitrarily normalized to aid in the comparison. Although good agreement in peak position of a high energy peak occurs (dashed line at 1128.2 eV in Fig. 1) differences of the Ga XAS of  $(\text{Ga}_x\text{Fe}_{1-x})_3\text{O}_4$  suggest that the actual local Ga bonding is not identical to the  $\beta$ - $\text{Ga}_2\text{O}_3$  structure, but more likely a substitution into Fe sites in the host  $\text{Fe}_3\text{O}_4$  spinel structure, similar to that determined in coprecipitation studies.<sup>1</sup> A definitive determination of the site occupancy of the Ga cannot be made from the Ga XAS spectra alone.

Indirect evidence for preference of the A-site or B-site substitution for the Ga dopant can be found in the Fe  $L_3$  XAS and XMCD. In the top panel of Fig. 2, the spectra for 0% gallium looks as expected for pure  $\text{Fe}_3\text{O}_4$ .<sup>12</sup> The primary peak at 709.25 dominates and the pre-edge is appropriately small. As

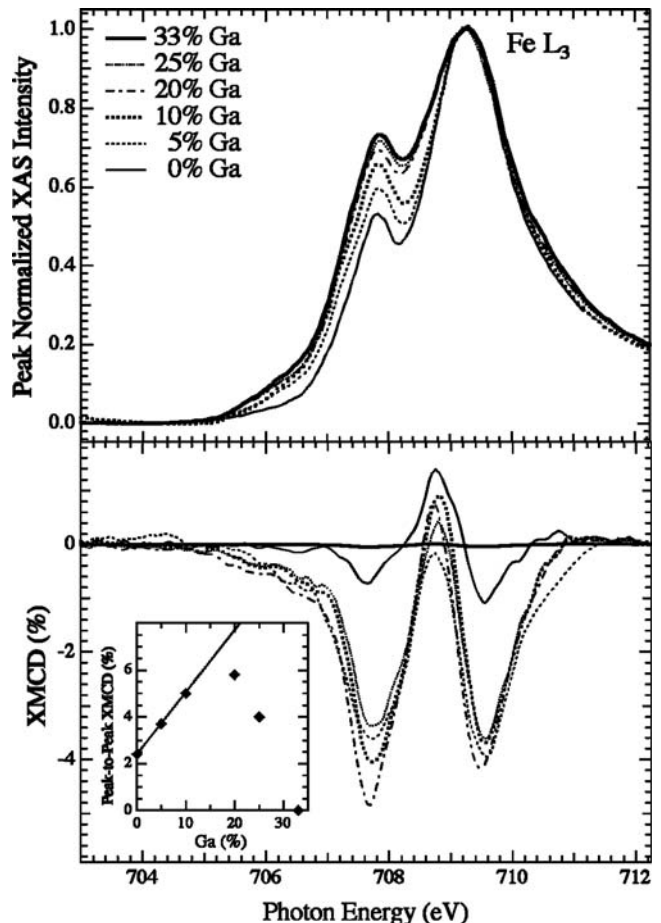


FIG. 2. XAS (top panel) and XMCD (bottom panel) of the Fe  $L_3$  edge for 0% (pure iron-oxide), 5%, 10%, and 20% Ga in  $\text{Fe}_3\text{O}_4$ . Bottom inset: The extracted peak-to-peak Fe XMCD intensity as a function of Ga concentration with a straight-line guide to the eye.

the amount of gallium increases the shoulder peak at 707.8 grows with respect to the primary peak. The growth of the shoulder peak at 707.8 is similar, indicative of an increase in the  $\text{Fe}^{2+}$  state in the octahedral coordination (B-site).<sup>12,13</sup>

This means that as the Ga substitutes into the spinel structure, it is not displacing the  $\text{Fe}^{2+}$  in the octahedral configuration so that the relative percentage of iron in this configuration is increasing. Given that the Ga XAS spectra is consistent with Ga in a 3+ valence (and in a tetrahedral coordination) and the Fe XAS data evidence that the iron is not removed from the octahedral 2+ coordination, the gallium appears to preferentially substitute into the tetrahedral  $\text{Fe}^{3+}$  A-site.

Dichroism spectroscopy (XMCD) is not only an excellent method of obtaining element-specific magnetic information but it also can be insightful in determining bonding configurations.<sup>13-15</sup> Examining the Fe  $L_3$  XMCD spectra for these nanoparticles (shown in the bottom panel of Fig. 2), the shape of the Fe XMCD spectra initially starts out with a mix of tetrahedral and octahedral coordination as one would expect of  $\text{Fe}_3\text{O}_4$ .<sup>13-15</sup> As the Ga percentage increases the central peak quickly reduces in prominence. As has been noted,<sup>13-15</sup> the intensity of this central peak is representative of the tetrahedral coordination, so the reduction of this peak is evidence of increasing octahedral coordination of Fe as opposed to the 1/3 tetrahedral to 2/3 octahedral mix of  $\text{Fe}_3\text{O}_4$ . In addition, comparing the relative intensities of the two downward peaks in the XMCD spectra, the lower energy peak is becoming more prominent as the concentration increases from 5% Ga to 25% gallium, which also indicates that the octahedral  $\text{Fe}^{2+}$  is becoming more dominant in the spectra at higher concentrations.

The observed increase in the Fe XMCD intensity is consistent with this picture. If the Ga is preferentially substituting into the tetrahedral A-site, then given the ferrimagnetic nature of the  $\text{Fe}_3\text{O}_4$  structure, substituting into the down spin site with a nonmagnetic dopant atom results in an overall increase in the moment per unit cell (as observed in the bulk for Zn doping). This is in fact observed as shown in the inset to Fig. 2. As the Ga is introduced the peak-to-peak dichroism signal increases up to 20% Ga. Due to the interplay between the three features present in the Fe  $L_3$  XMCD spectra, a quantitative extraction of the moment per Fe atom must be performed carefully with modeled spectra.

## IV. CONCLUSIONS

Gallium doped iron oxide spinel nanoparticles of average size 8.75 nm have been synthesized and demonstrate weak interparticle interactions expected of such particles. The Ga is found to preferentially substitute into the tetrahedral A-site of the  $\text{Fe}_3\text{O}_4$  spinel structure as a 3+ ion. This can be seen clearly in the Fe  $L_3$  XAS and XMCD spectra and is supported by the observed magnetization trend. The doping of Ga as 3+ in the tetrahedral configuration causes the moment per iron atom of the particles to increase with increasing Ga concentration until 20% Ga, after which the nonmagnetic nature of Ga causes the moment to quickly fall to 0 in a manner similar to other dopant materials in bulk  $\text{Fe}_3\text{O}_4$ .

## ACKNOWLEDGMENTS

This work is supported by the National Science Foundation under Grant No. CBET-0709358. The ALS is supported by the U.S. Department of Energy under Contract No. DEAC02-05CH11231.

- <sup>1</sup>J. M. G. Amores, V. S. Escridano, G. Busca, E. F. Lopez, and M. Saidi, *J. Mater. Chem.* **11**, 3234 (2001).
- <sup>2</sup>V. Kanazirev, R. Dimitrova, G. L. Price, A. Yu. Kodakov, L. M. Kustov, and V. B. Kazensky, *J. Mol. Catal.* **70**, 111 (1990).
- <sup>3</sup>V. Kanazirev, G. L. Price, and M. Dooley, *J. Chem. Soc., Chem. Commun.* **9**, 712 (1990).
- <sup>4</sup>P. Meriaudeau, G. Sapaly, and C. Naccache, *J. Mol. Catal.* **81**, 293 (1990).
- <sup>5</sup>E.W. Gorter, *Philips Res. Rep.* **9**, 351 (1954).
- <sup>6</sup>S. Sun and H. Zeng, *J. Am. Chem. Soc.* **124**, 8204 (2002).
- <sup>7</sup>E. Tronc, D. Fiorani, M. Noguès, A. M. Testa, F. Lucari, F. D'Orazio, J. M. Grenèche, W. Wernsdorfer, N. Galvez, C. Chanéac, D. Mailly, and J. P. Jolivet, *J. Magn. Magn. Mater.* **262**, 6 (2003).
- <sup>8</sup>S. Ammar, N. Jouini, F. Fiévet, O. Stephan, C. Marhic, M. Richard, F. Villain, Ch. Cartier dit Moulin, S. Brice, and Ph. Sainctavit, *J. Non-Cryst. Solids* **658**, 345 (2004).
- <sup>9</sup>V. L. Pool, M. T. Klem, J. Holroyd, T. Harris, E. Arenholz, M. Young, T. Douglas, and Y. U. Idzerda, *J. Appl. Phys.* **105**, 07B515 (2009).
- <sup>10</sup>T. J. Regan, H. Ohldag, C. Stamm, F. Nolting, J. Lüning, J. Stöhr, and R. L. White, *Phys. Rev. B* **64**, 214422 (2001).
- <sup>11</sup>V. Pool, M. Klem, C. Jolley, E. A. Arenholz, T. Douglas, M. Young, and Y. U. Idzerda, *J. Appl. Phys.* **107**, 09B517 (2010).
- <sup>12</sup>H.-J. Kim, J.-H. Park, and E. Vescovo, *Phys. Rev. B* **61**, 15284 (2000).
- <sup>13</sup>F. Schedin, E.W. Hill, G. Van der Laan, and G. Thornton, *J. Appl. Phys.* **96**, 1165 (2004).
- <sup>14</sup>S. Brice-Profeta, M.-A. Arrio, E. Tronc, I. Letard, Ch. Cartier dit Moulin, and Ph. Sainctavit, *Phys. Scr.*, T **115**, 626 (2005).
- <sup>15</sup>J.-S. Kang, G. Kim, H. J. Lee, D. H. Kim, H. S. Kim, J. H. Shim, S. Lee, H. Lee, J.-Y. Kim, B. H. Kim, and B. I. Min, *Phys. Rev. B* **77**, 035121 (2008).

## **DISCLAIMER**

This document was prepared as an account of work sponsored by the United States Government. While this document is believed to contain correct information, neither the United States Government nor any agency thereof, nor the Regents of the University of California, nor any of their employees, makes any warranty, express or implied, or assumes any legal responsibility for the accuracy, completeness, or usefulness of any information, apparatus, product, or process disclosed, or represents that its use would not infringe privately owned rights. Reference herein to any specific commercial product, process, or service by its trade name, trademark, manufacturer, or otherwise, does not necessarily constitute or imply its endorsement, recommendation, or favoring by the United States Government or any agency thereof, or the Regents of the University of California. The views and opinions of authors expressed herein do not necessarily state or reflect those of the United States Government or any agency thereof or the Regents of the University of California.